INTERNATIONAL JOURNAL OF GEOMETRY
Vol. 11 (2022), No. 1, 54 - 77

SIMILARITIES RELATED TO PIVOTING AND BROCARD POINTS

PARIS PAMFILOS

Abstract In this article we study the similarities of triangles $A_\varphi B_\varphi C_\varphi$ pivoting inside another triangle ABC. In particular we determine the geometric locus of the similarity centers of the pivoting triangle $A_\varphi B_\varphi C_\varphi$ and an arbitrary third triangle $A'B'C'$ of the same similarity type located at an arbitrary place of the plane. It is shown that in the case of direct similarities the locus is a circle and in the case of indirect- or anti- similarities the locus is a conic. These results are applied to the case of Brocard points as well as the other pivots of the triangle ABC producing pivoting triangles similar to ABC. In this case the circles involved are the *"orthocenroidal"* and the circumcircle, whereas the conics are three hyperbolas and two *"triangle conics"* passing through the vertices and the Tarry point of the triangle.

1 Introduction

The *"pedal $\tau_0 = \triangle A_0B_0C_0$ of a point P w.r.t the triangle $\tau = ABC$"* is defined by the orthogonal projections of P on the sides of τ (see figure 1-(I)). We say that the pedal τ_0 is *inscribed* in τ. More general we say that a triangle $\tau' = A'B'C'$ *"is inscribed"* in τ if the vertices of τ' lie on corresponding sides of τ.

A basic property of the pedal is the one suggested by figure 1-(II). If we turn the

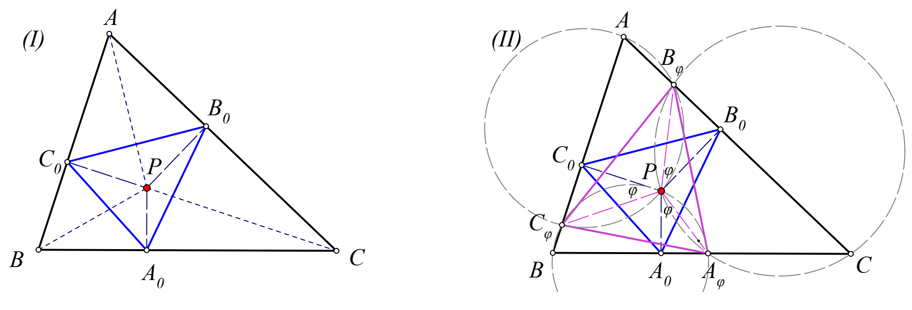

Figure 1: The pedal $\triangle A_0B_0C_0$ of P w.r.t $\triangle ABC$

segments $\{PA_0, PB_0, PC_0\}$ by the same oriented angle φ and consider the new positions $\{A_\varphi, B_\varphi, C_\varphi\}$ on the sides, then the created right angled triangles $\{PA'A_\varphi, PB'B_\varphi, PC'C_\varphi\}$

Keywords and phrases: Brocard, Triangle, Transformation, Similarity, Conics
(2020)Mathematics Subject Classification: 51M15, 51N15, 51N20, 51N25
Received: 06.04.2021. In revised form: 25.09.2021. Accepted: 24.11.2021

are similar and the triangle $\tau_\varphi = A_\varphi B_\varphi C_\varphi$ is similar to the pedal τ_0. Thus, a point P defines the pedal triangle and also an *infinitude of similar to it triangles* having their vertices on corresponding sides of the triangle of reference. Obviously the pedal triangle τ_0 is the *"smallest"* among all these similar triangles and there is no *"biggest"*, since, for φ tending to $\pi/2$ the segment PA_φ tends to become parallel to BC and its length tends to infinity. For all these triangles we say that they *"pivot"* about P and point P is called *"pivot center"* or simply *"pivot"*.

We notice that any one of the triangles τ_φ pivoting about P determines point P as intersection of the three circles:

$$(A_\varphi B_\varphi C) \ , \ (B_\varphi C_\varphi A) \ , \ (C_\varphi A_\varphi B) \, .$$

In fact, by the well known Miquel theorem ([16, p.79], [17, p.131]), any three points A_φ, B_φ, C_φ on respective sides of the triangle τ define the preceding three circles passing through a common point P, the *"Miquel point"* of the triple $\{A_\varphi, B_\varphi, C_\varphi\}$ relative to τ (see figure 1-(II)). It is also easily seen, that drawing the perpendiculars $\{PA_0, PB_0, PC_0\}$ to respective sides of τ we obtain the pedal τ_0 of P with the same angles as τ_φ.

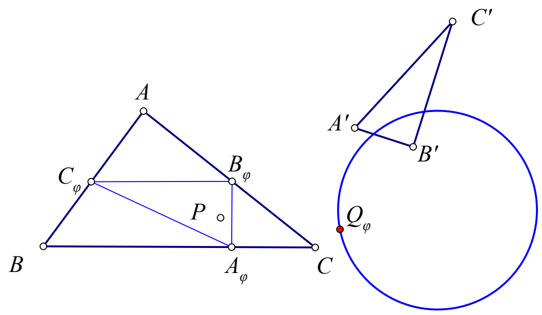

Figure 2: Locus of similarity centers $\{Q_\varphi\}$ of direct similarities $\{f_\varphi : \tau_\varphi \mapsto \tau'\}$

In this article we consider a pivoting triangle τ_φ of τ about the arbitrary but fixed point P and a third fixed triangle $\tau' = A'B'C'$ of the similarity type of τ_φ. We invetigate the locus of the centers Q_φ of the similarities f_φ mapping the pivoting τ_φ to τ' (which are the same with the centers of their inverses f_φ^{-1}). It turns out that these centers describe circles in the case f_φ are *"direct"* similarities (see Figure 2). In the case of *"indirect"* or

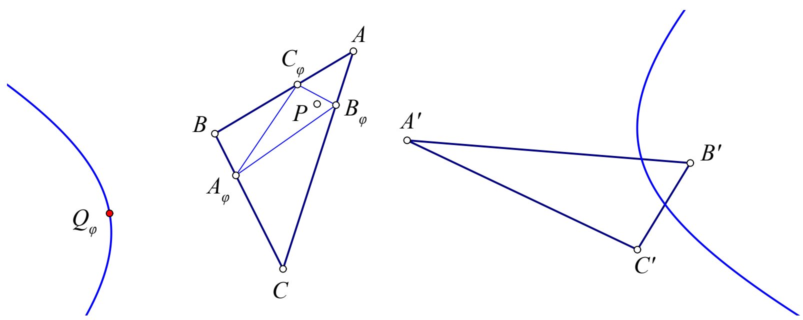

Figure 3: Locus of centers $\{Q_\varphi\}$ of anti-similarities $\{f_\varphi : \tau_\varphi \mapsto \tau'\}$

"anti-similarities", in which all the triangles τ_φ are oppositely oriented to $\tau' = A'B'C'$, the similarity centers Q_φ describe a conic (see Figure 3). The material is organized as follows.

In section 2 we review some necessary for our discussion results about similarities and pivoting. In section 3 we prove the validity of the aforementioned claims. In section 4 we review the configuration of the 12 pivots producing pivoting triangles of the same similarity type. In section 5 we apply these results to the case of pivots, which, like the Brocard points, produce pedals similar to the triangle of reference τ. The subsequent sections 6-9 contain the main results of this article. It turns out, that, besides the two Brocard points, the other pivots generate geometric loci consisting of two circles, three hyperbolas and two triangle conics intimately related to the triangle of reference.

2 Similarity centers

"Similarities" are transformations f of the plane, which multiply the distances $|XY|$ of points by a constant $k > 0$, called *"ratio"* or *"scale"*. By definition then, for every pair of points $\{X, Y\}$ a similarity corresponds points

$$X' = f(X), \; Y' = f(Y), \quad \text{which satisfy} \quad |X'Y'| = k \cdot |XY|.$$

This general definition includes the *"isometries"* or *"congruences"*, for which $k = 1$, and the *"homotheties"*. Simillarities not coincident with isometries, in other words, similarities for which $k \neq 1$ are called *"proper"* and are divided into two categories: *"direct"* or *"rotational"* and *"indirect"* or *"antisimilarities"* or *"reflective"* similarities ([6, p.67], [28, vol.II], [1, p.217], [23]).

A *"direct"* or *"rotational"* similarity is defined as a composition $g \circ f$ of a rotation f and a homothety g, which shares the same center with f. The rotation angle of f is called *"angle"* of similarity. An *"antisimilarity"* is defined as a composition $g \circ f$ of a reflection f and a homothety g with center on the axis of f, called *"axis"* of the antisimilarity. It is easily seen that the order of the transformations, which participate in this definition, is irrelevant and there exists a unique point, the center O of the homothety g, called *"center"* of the similarity which is fixed under the transformation.

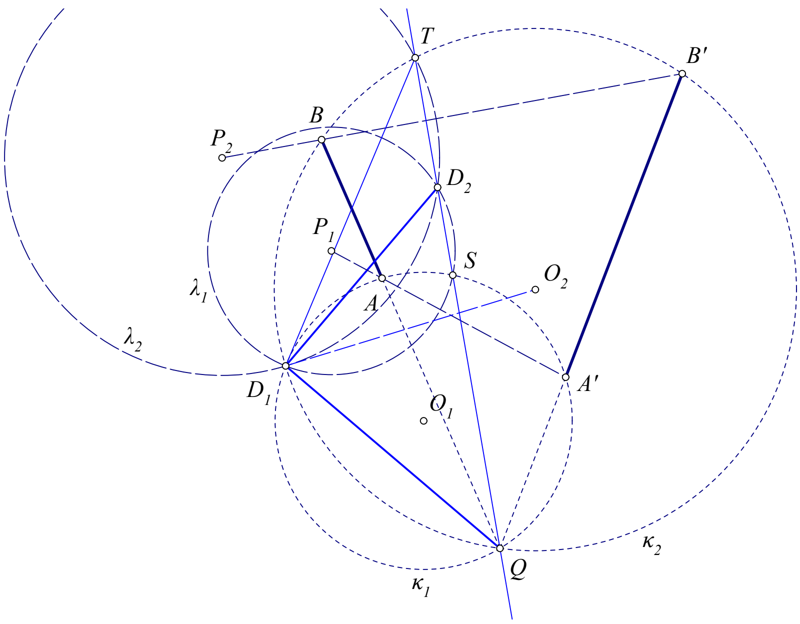

Figure 4: The centers $\{D_1, D_2\}$ of the two similarities mapping AB onto $A'B'$

Figure 4 illustrates some basic facts about the similarities relating two line segments $\{AB, A'B'\}$ in general position. It is well known that for two such segments there is exactly one direct and one indirect similarity mapping AB onto $A'B'$. The proofs of this fact and of the next theorem indicating the relative position of the similarity centers can be found in [23]. The circles $\{\kappa_1 = (AA'Q), \kappa_2 = (BB'Q)\}$ are directly defined from the two given segments and the intersection point of their supporting lines $Q = AB \cap A'B'$. The circles $\{\lambda_1, \lambda_2\}$ are the Apollonian circles ([5, p.15]) respectively of $\{AA', BB'\}$ relative to the ratio $k = AB/A'B'$. Their intersections are the two similarity centers. From the center D_1 of the direct similarity pass all four circles, whereas from the center D_2 of the antisimilarity pass only the two Apollonian circles. Of some importance are also the intersection points of the circles $\{S = \kappa_1 \cap \lambda_1, T = \kappa_2 \cap \lambda_2\}$.

Theorem 1. *Under the preceding conventions and notation, the following are valid properties.*

1. *Triangles $\{ASA', BTB'\}$ are similar.*
2. *Points $\{T, S, Q\}$ are collinear.*
3. *D_2 is collinear with $\{T, S, Q\}$.*
4. *The angle $\widehat{D_2D_1Q}$ is right.*
5. *The lines $\{QD_1, QD_2\}$ are harmonic conjugate w.r.t. $\{AB, A'B'\}$.*

Remark 1. The fact, that the similarity is uniquely defined from two corresponding segments, reduces the study of a concrete similarity of two plane shapes to the induced similarity on an arbitrary pair of corresponding, under the similarity, segments of these shapes. Thus, in the case of similar triangles, their similarity can be studied by considering the induced similarity on two corresponding sides of them or the similarity of two other corresponding segments of them, like, for example, the segments on each triangle joining the circumcenter with a corresponding under the similarity vertex.

3 Relations to Moebius and quadratic transformations

Referring to figure 5, in our discussion we'll consider a fixed segment $A'B'$ and a segment AB with fixed end point A and variable B. For each position of B we obtain, as explained in the preceding section, two similarities, direct and indirect, mapping the variable AB onto the fixed $A'B'$ and two corresponding similarity centers $\{D_1, D_2\}$. This creates two maps $f_1 : B \mapsto D_1$ and $f_2 : B \mapsto D_2$ lying on the basis of our investigation. We'll show that f_1 is a Moebius transformation ([7], [26]) and f_2 is a *"quadratic"* transformation ([27, p.19], [13, p.329]) mapping lines to conics. This results from two simple facts. The first follows directly from the definition of the similarity and guarantees the similarity of the triangles $\{D_1AB \sim D_1A'B'\}$ and $\{D_2AB \sim D_2A'B'\}$. The second fact is a well known representation of the similarity of two triangles using complex numbers which I formulate as a lemma without proof ([7, p.137, p.176], [15, p.59]).

Lemma 1. *Representing the vertices of the triangles $\{ABC, A'B'C'\}$ with complex numbers, and denoting by $\overline{A}$ the conjugate of A, the similarity of the triangles is expressed by the vanishing of two complex determinants:*

$$\textit{direct:}\ \begin{vmatrix} A' & A & 1 \\ B' & B & 1 \\ C' & C & 1 \end{vmatrix} = 0 \quad \textit{and} \quad \textit{antisimilarity:}\ \begin{vmatrix} A' & \overline{A} & 1 \\ B' & \overline{B} & 1 \\ C' & \overline{C} & 1 \end{vmatrix} = 0. \tag{1}$$

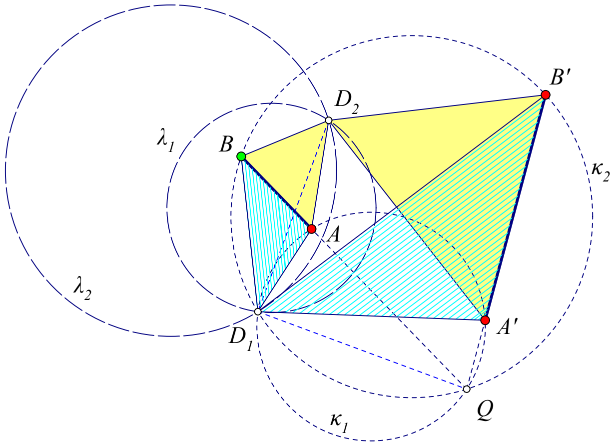

Figure 5: Triangles $D_1AB \sim D_1A'B'$ and $D_2AB \sim D_2A'B'$

Applying this to the similar triangles $\{D_1AB, D_1A'B'\}$ (see Figure 5) we obtain

$$\begin{vmatrix} D_1 & D_1 & 1 \\ A' & A & 1 \\ B' & B & 1 \end{vmatrix} = 0 \quad \Leftrightarrow \quad D_1 = \frac{A \cdot B' - A' \cdot B}{(B' - A' + A) - B}, \tag{2}$$

showing that $D_1 = f_1(B)$ is indeed a Moebius transformation, mapping every line not passing through its pole $B' - A' + A$ to a circle. Notice that $\{A, B'\}$ are the *"fixed"* points of the transformation and the pole $B_0 = B' - A' + A \Leftrightarrow B_0 - A = B' - A'$ defines two equal and parallel segments $\{AB_0, A'B'\}$ and the *"characteristic parallelogram"* $AB_0B'A'$ of the Moebius transformation ([26, p.69]). Point A' is the image of the point at infinity or the pole of the inverse Moebius transformation. This implies that every line not passing through the pole B_0 maps to a circle through the point A'.

Doing the analogous work for the antisimilar triangles $\{D_2AB, D_2A'B'\}$ we obtain

$$\begin{vmatrix} D_2 & \overline{D_2} & 1 \\ A' & \overline{A} & 1 \\ B' & \overline{B} & 1 \end{vmatrix} = 0\,. \tag{3}$$

Expanding the determinant and equating its real and imaginary parts to zero, we find indeed two rational quadratic functions expressing D_2 in terms of the variable B and the constants $\{A, A', B'\}$. To avoid excessive computations and see the form of these equations it suffices to use a similarity and reduce the configuration to one having $\{A' = 1, B' = 0\}$, leading to the following relations for $\{D_2 = d_1 + i \cdot d_2\,,\ A = a_1 + i \cdot a_2\,,\ B = x + i \cdot y\}$:

$$\begin{aligned} d_1 &= \frac{x^2 + y^2 - (a_1 + 1)x - a_2 y}{(x - a_1)^2 + (y - a_2)^2 - 1}, \\ d_2 &= \frac{(a_1 - 1)y - a_2 x}{(x - a_1)^2 + (y - a_2)^2 - 1}. \end{aligned} \tag{4}$$

Figure 6 shows the ingredients involved in the construction of this quadratic transformation f_2. $\{\kappa_1, \kappa_2\}$ are the circle and the line represented by the nominators of $\{d_1, d_2\}$. κ_3 is the circle represented by their common denominator. The figure shows the image $\varepsilon' = f_1(\varepsilon)$ of a line ε, a conic passing through the point A' attained when (x, y) goes to infinity. Point C is the common one to the three curves $\{\kappa_1, \kappa_2, \kappa_3\}$ and one of the *"base*

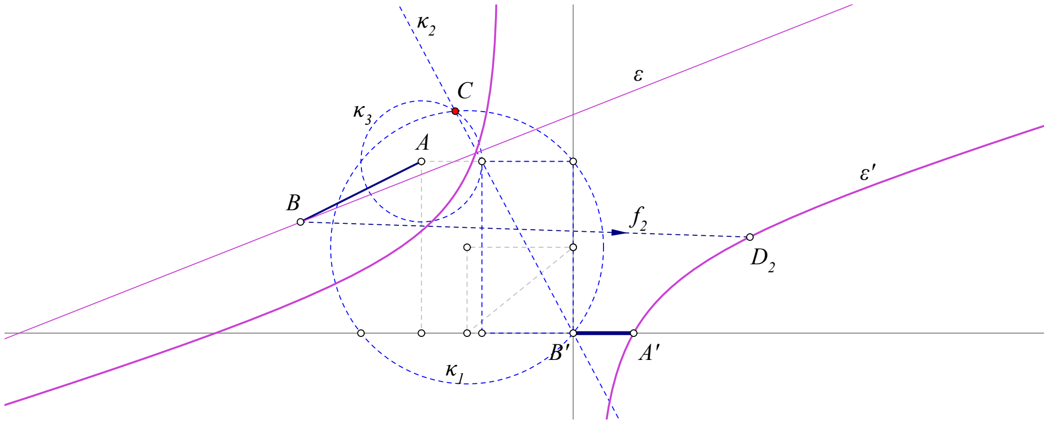

Figure 6: The transformation f_1 and the conic $\varepsilon' = f_1(\varepsilon)$ for a line ε

points" of the quadratic transformation ([13, p.329]), the other two being the *"cyclic points at infinity"* ([19, II, p.162], [9, p. 204]). As it happens for every quadratic transformation, the base points are contained in every pre-image $f_2^{-1}(\varepsilon)$ of a line ε of the plane. The pre-images of lines, equivalently images of lines via f_2^{-1}, are circles through C (and the cyclic points at infinity). In fact, the pre-image of the line $ax + by + c = 0$ is obtained by replacing $\{d_1, d_2\}$ in $ad_1 + bd_2 + c = 0$ by the expressions in (4) and it is readily seen that the resulting equation represents a circle passing through C. We formulate the essentials of these facts in the following theorem.

Theorem 2. *Given two line segments $\{AB, A'B'\}$ in general position and considering $\{A, A', B'\}$ fixed and variable the end point B of the first segment, we obtain for each B two similarities mapping AB onto $A'B'$: the direct similarity with center D_1 and the antisimilarity with center D_2. The correspondence $f_1 : B \mapsto D_1$ is a Moebius transformation mapping lines, not passing through its pole $B_0 = B' - A' + A$, to circles through point A'. The correspondence $f_2 : B \mapsto D_2$ is a quadratic transformation mapping lines to conics through the point A'.*

4 The 12 pivots configuration

Behind the pivoting configuration of a triangle $A'B'C'$ in the triangle ABC there are two basic relations between the angles appearing there and resulting by a simple angle chasing argument (see Figure 7):

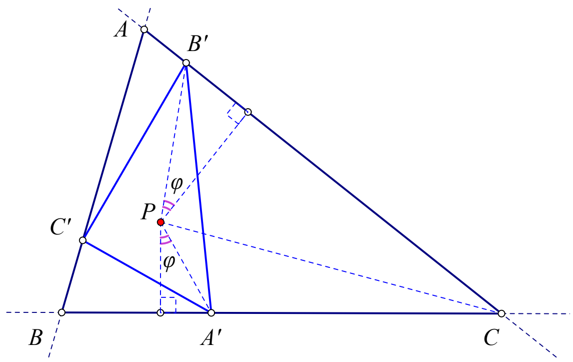

Figure 7: The transformation f_1 and the conic $\varepsilon' = f_1(\varepsilon)$ for a line ε

$$\widehat{PA'B'} = \widehat{PCB'} \ , \ \widehat{PB'A'} = \widehat{PCA'} \quad \text{and} \quad \widehat{A'PB'} = \pi - \widehat{C},$$
$$\widehat{BPC} = \widehat{A} + \widehat{A'} \ , \ \widehat{CPA} = \hat{B} + \widehat{B'} \ , \ \widehat{APB} = \widehat{C} + \widehat{C'} \ . \tag{5}$$

The second is valid for points P lying inside the triangle, but it is also general valid if we interpret the angles as *"directed angles"*, in the sense discussed by Johnson ([17, p.133]).

A basic fact about pedals is their *"invariance of similarity type under inversions"* ([17, p.140]). Thus, fixing a point P and considering its inverses w.r.t. the four inversions that leave the triangle ABC invariant we obtain several other points defining pedals of the same similarity type. The aforementioned four inversions are (i) the inversion w.r.t. the circumcircle and (ii) the inversions w.r.t. to the three Apollonian circles ([5, p.260]) of the triangle ABC. It is well known ([25]), that fixing P and applying these inversions repeatedly we obtain in general twelve points which have a pedal similar to that of P and these are all the points of the plane having this property. Each one of the twelve pivots is distinguished by the information: (i) which vertex of the pivoting triangle glides on a side of the fixed triangle and (ii) the orientation of the pivoting relative to the fixed triangle. For the combination {vertex of pivoting $\leftrightarrow$ side of fixed} there are six possibilities. Each one of the six can be realized by equally or oppositely oriented triangles, thus leading to the aforementioned twelve possible pivot centers.

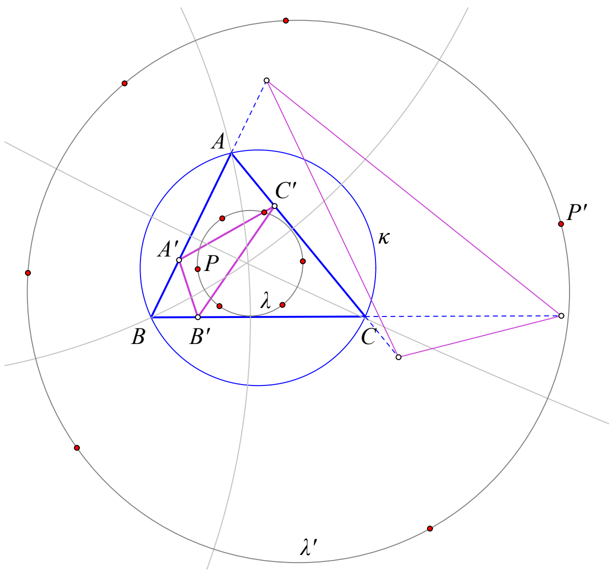

Figure 8: Twelve pivots

Figure 8 shows a typical case of the pedal $\triangle A'B'C'$ of the point P w.r.t. $\triangle ABC$ and also the remaining eleven other points producing a pedal similar to $\triangle A'B'C'$. It contains also the pedal of another P' of these points with pedal similar to $\triangle A'B'C'$. Any one of the twelve points produces the others by applying to it successively some of the aforementioned inversions. Also the twelve points lie by 6 on two *"Schoute"* circles $\{\lambda, \lambda'\}$, i.e. circles orthogonal to the pencil generated by the Apollonian circles ([17, p.299]) and permuted by the inversion w.r.t. the circumcircle κ of $\triangle ABC$. The inversions w.r.t. to the Apollonian circles preserve every Schoute circle, hence permute the six pivots of each Schoute circle containing them without to mix points of different circles. The pencil of Apollonian circles of a triangle is an intersecting one, the two intersection (base) points being the *"isodynamic"* points of the triangle ([5, p.262]). The Schoute pencil being orthogonal to the Apollonian pencil is of non-intersecting type and contains the circumcircle of $\triangle ABC$, whose inversion interchanges the two Schoute circles carrying the twelve pivots.

Thus, we can speak of the six *"inner pivots"* lying on the Schoute circle λ inside the circumcircle κ and the *"outer"* pivots lying on the Schoute circle λ' outside the circumcircle.

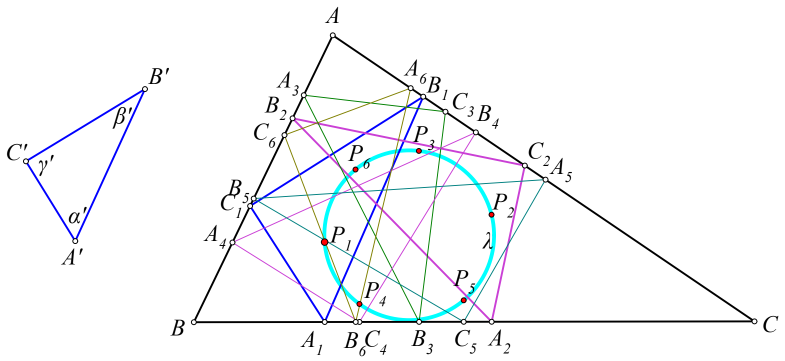

Figure 9: Six *"inner"* pivots defining pedals of $\triangle ABC$ similar to $\triangle A'B'C'$

Figure 9 shows a typical case of the six *inner* pivots and their corresponding pedals similar to $\triangle A'B'C'$. In the sequel we call such a set of twelve pivots a *"12 pivots configuration"*.

5 The Brocard 11 pivots configuration

The *"Brocard 11 pivots configuration"* is characterized by the property of its pivots, to define pedals similar to the fixed triangle of reference ABC. Thus, it contains the two Brocard points ([5, p.274]) and several others, among them the prominent one: the circumcenter O of $\triangle ABC$, whose pedal is the *"complementary"* $\triangle A'B'C'$ with vertices the middles of the sides of $\triangle ABC$ (see Figure 10). Because of this, the Brocard configuration is the unique

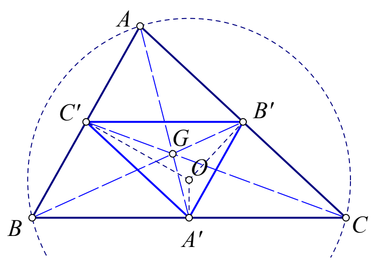

Figure 10: The complementary $\triangle A'B'C'$ of $\triangle ABC$

one containing ... only 11 instead of 12 real pivots. The reason for this loss is that the inverse of O w.r.t. the circumcircle $\kappa(O)$ of $\triangle ABC$, which is also one of the 12 pivots, is the point at infinity and does not define a genuine finite pedal triangle.

Figure 11 shows the two Brocard points $\{\Omega, \Omega'\}$ of ABC together with the other possible points whose pedals are similar to the triangle of reference ABC. Six of these points lie on the *"Brocard circle"* of the triangle, i.e. the (inner) Schoute circle through the circumcenter. The other six are inverses of the former and lie on the *"Lemoine axis"*, which is the $\kappa-$inverse of the Brocard circle of the triangle (outer Schoute circle).

The six points on the Brocard circle are: the circumcenter O, the two Brocard points $\{\Omega, \Omega'\}$ and the inverses $\{A_2, B_2, C_2\}$ of O w.r.t. the Apollonian circles $\{\lambda_A, \lambda_B, \lambda_C\}$, coinciding with the vertices of the *"second Brocard triangle"* ([17, p.279]).

The six other points are the $\kappa-$inverses of the former and lie on the Lemoine axis. Disregarding the point at infinity which is the $\kappa-$inverse of O, two of the points are the

$\kappa-$inverses $\{\Omega^*, \Omega'^*\}$ of the Brocard points and the other three $\{A_2', B_2', C_2'\}$ on the axis are the centers of the Apollonian circles $\{\lambda_A, \lambda_B, \lambda_C\}$. Our main concern in this article is to

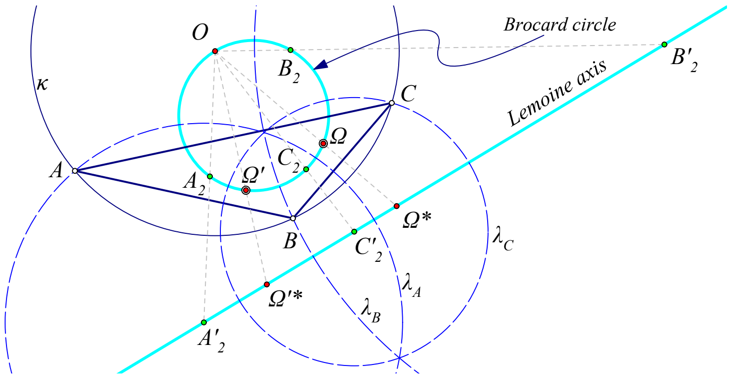

Figure 11: The Brocard 11 pivots configuration

study, for each one of these 11 points, the pivoting triangles $A'B'C'$ about that point and find the geometric locus of the centers of the similarities mapping $\triangle ABC$ onto $A'B'C'$.

Figure 12 shows some of the triangles pivoting about the first Brocard point Ω. This is the simplest case in this context and in some sense unimportant, since the aforementioned similarity centers coincide with Ω for all triangles pivoting about Ω. This is even a characteristic of the Brocard points $\{\Omega, \Omega'\}$ among the 11 pivots producing triangles

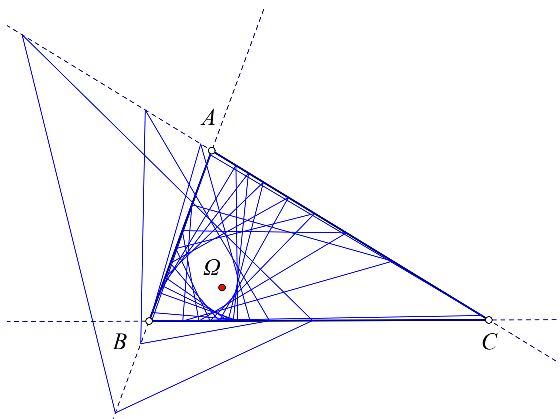

Figure 12: Triangles similar to $\triangle ABC$ pivoting about the first Brocard point Ω

similar to $\triangle ABC$. In fact, it can be easily proved that the similarity mapping $\triangle ABC$ to a triangle $A'B'C'$ pivoting about Ω has its center at Ω ([17, p.394]), the same property holding also for Ω'. This is not true for the other 9 pivots of the Brocard configuration. A counterexample is suggested by figure 10 of the complementary triangle, which is similar to ABC but the corresponding similarity center is obviously the centroid G, which is different from the pivot O when the triangle is non equilateral. Below we take a closer look into this case.

Before to enter into the details of the similarities we notice, that since all pivots of the Brocard configuration are obtained from the circumcenter O by successive inversions, and inversions reverse the orientation, the pivots fall into two classes, depending on the number of inversions needed: odd or even. Thus it is easily seen (see Figure 11) that $\{O, \Omega, \Omega', A_2', B_2', C_2'\}$ are pivots with positively oriented pedals and $\{\Omega^*, \Omega'^*, A_2, B_2, C_2\}$ are pivots with negatively oriented pedals. We'll see that this difference is reflected also to the corresponding geometric loci of the similarity centers. The loci for the first set are circles and for the second set are conics.

6 Pivoting about the circumcenter

In this section we consider the pivoting $\tau' = A'B'C'$ of the pedal triangle of triangle $\tau = ABC$ w.r.t. the circumcenter O of τ. This pedal or *"complementary"* of τ is similar to τ and the same is true for all the triangles τ' pivoting about O. The center Q of the similarity of the two triangles $\{\tau, \tau'\}$ (see Figure 13) is the same with the center of of

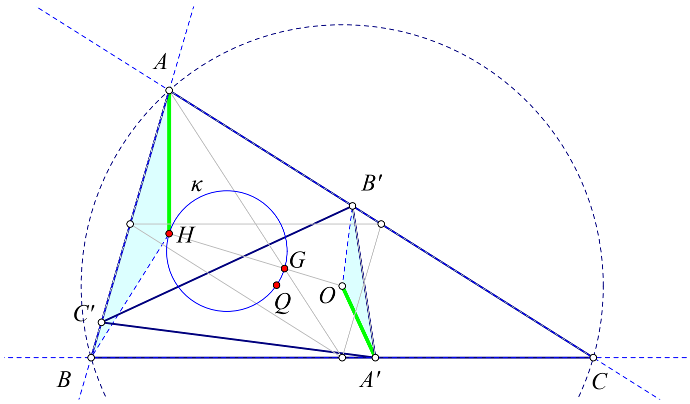

Figure 13: Reduction of the similarity to that of two segments

similarity of the partial triangle $OA'B'$ to the triangle HAB, where H is the orthocenter of τ. This, because the similarity transforming $\triangle OA'B'$ to $\triangle HAB$ transfrorms also τ' to τ and vice versa. For the same reason latter similarity coincides with the one transforming the oriented segment OA' to HA. Next theorem formulates the result of these observations.

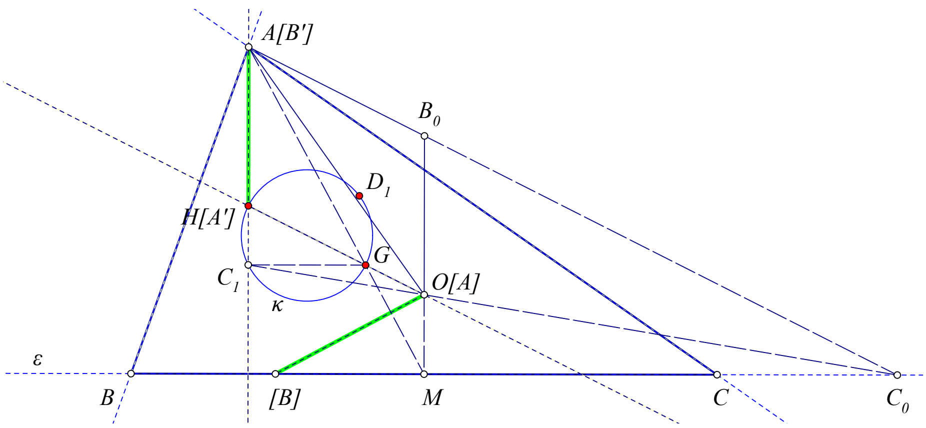

Figure 14: The center D_1 of the similarity mapping $O[B]$ to HA

Theorem 3. *The similarity center Q of the pivoting triangle $\tau' = A'B'C'$ about the circumcenter and the triangle of reference $\tau = ABC$ lies on the circle κ with diameter HG, where $\{H, G\}$ are respectively the orthocenter and the centroid of the triangle.*

Proof. The proof (see Figure 14) results by applying theorem 2. The labels in brackets of figure 14, indicate the correspondence with the notation of this theorem. The requested geometric locus of the center D_1 of the similarity mapping $[AB]$ onto $[A'B']$ is a circle κ passing through $[A']$. For this it suffices to verify that the pole $B_0 = [A + (B' - A')]$ of the Moebius transformation $f_1 : [B] \mapsto D_1$ is not contained in the line $\varepsilon = BC$ on which $[B]$ varies, which is trivial. It is also easy to verify that the centroid G belongs to the locus. A third point which is also easily seen to belong to the locus is the intersection $C_1 = OC_0 \cap HA$ with $C_0 = BC \cap AB_0$ defining the trapezium $AHOC_0$. The angle $\widehat{GC_1H}$ is easily seen to be a right one and this completes the proof of the theorem. □

Remark 2. The circle with diameter HG is traditionally called *"orthocentoidal"* circle of the triangle ABC ([3, p.436], [8], [10]). It is known ([14]), that *the incenter of a nonequilateral triangle lies inside this circle and all the excenters lie outside it* and also ([2]), that *one only of the Brocard points lies inside this circle and if it is on this circle, then both Brocard points are on this circle and the triangle is isosceles.*

Remark 3. Notice that the position of D_1 on κ uniquely determines the similarity of $\triangle ABC$ to the corresponding inscribed triangle $A'B'C'$ in $\triangle ABC$ since, except the center of similarity, we have also its angle $\widehat{HD_1O}$ and its ratio D_1H/D_1O.

7 Pivoting about an Apollonian center

Besides the Brocard points and the circumcenter, the other pivots of triangles $\{A'B'C'\}$ directly similar to the triangle of reference ABC are the centers $\{A_2', B_2', C_2'\}$ of the three Apollonian circles $\{\lambda_A, \lambda_B, \lambda_C\}$. Here the situation becomes significantly simpler because one of the projections on the sides of such a pivot, A_2' say, is the pivot itself $A' = A_2'$, since it is contained in the side BC of the triangle (see Figure 15).

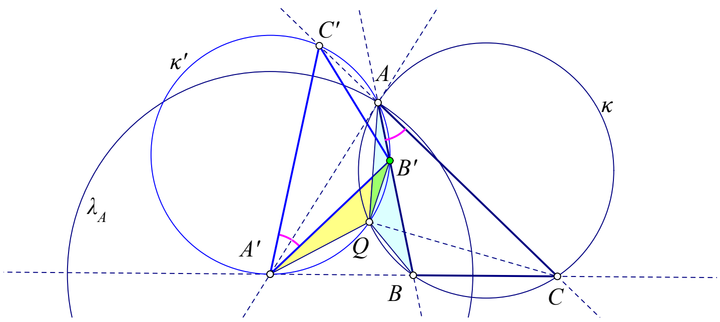

Figure 15: Centers Q of similarities mapping the pivoting $\triangle A'B'C'$ to $\triangle ABC$

Theorem 4. *The centers Q of the similarities mapping the pivoting triangles $A'B'C'$ about an Apollonian center to the triangle of reference ABC are on the circumcircle κ of $\triangle ABC$.*

Proof. We discuss the case of the center $A' = A_2'$ of the Apollonian circle λ_A passing through A. The other cases are completely analogous to this one. In this case the pivoting triangle $A'B'C'$ has a circumcircle κ' passing through A and intersecting a second time the circumcircle κ of $\triangle ABC$ at a point Q. This is the similarity center. To see this it suffices to prove that the triangles $\{AQB, A'QB'\}$ are similar (see Figure 15). This follows by a simple angle chasing argument considering the cyclic quadrangles $\{AQBC, A'QB'C'\}$ and taking into account that the tangent to κ at A passes through A' :

$$\widehat{AQB} = \widehat{A'QB'} \quad \text{and} \quad \widehat{QBA} = \widehat{QCA} = \widehat{QAA'} = \widehat{QB'A'} \,. \qquad \square$$

8 Pivoting about a vertex of the second Brocard triangle

Before to start the investigation of the corresponding locus I include a theorem on well known facts, useful in the sequel, about the vertices of the second Brocard triangle $A_2B_2C_2$, their proofs to be found in [24]. The isogonal conjugates of the vertices of the second Brocard triangle, like the point D_A appearing below, are the vertices of the *"fourth Brocard triangle"* ([12]).

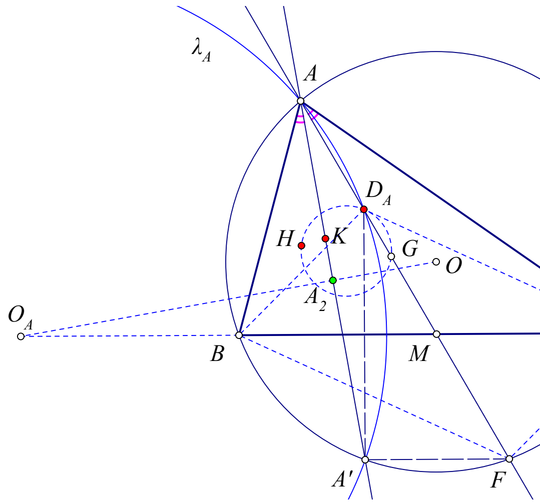

Figure 16: The projection A_2 of O on the symmedian AK

Theorem 5. *Referring to figure 16, we denote by $\kappa(O)$ the circumcircle of $\triangle ABC$ and consider the points: the second intersection A' of the symmedian AK with κ, the second intersection F of the median AM with κ and the reflection D_A of A' in BC.*

1. *$BA'FC$ is a trapezium and $A'F$ is parallel to BC.*
2. *Point A' is on the Apollonian circle $\lambda_A(O_A)$, satisfying $A'B/A'C = b/c$.*
3. *Point A_2 is the middle of AA', line OA_2 passes through O_A.*
4. *Point A_2 is the inverse of O w.r.t. to λ_A.*
5. *Point D_A is the second intersection of the Apollonian circle λ_A with the median AM.*
6. *D_ABFC is a parallelogram and point D_A is the isogonal conjugate of A_2.*
7. *Point D_A is on the orthocentroidal circle with diameter GH.*

Corollary 1. *As the triangle $A'B'C'$ pivots about A_2 the triangle $A_2A'B'$ remains similar to D_AAC and the antisimilarity mapping $\triangle A'B'C'$ to $\triangle ABC$ maps also $\triangle A_2A'B'$ to D_AAC.*

Proof. This is easily seen by considering the pedal of A_2 to which all the pivoting $\triangle A'B'C'$ are directly similar. Their partial triangle $A_2A'B'$ remains by the pivoting similar to the corresponding triangle of the pedal. On the other side considering the partial triangle of this pedal (see Figure 17), we see that the angle $\widehat{A_2B'A'} = \widehat{A_2CA'} = \widehat{D_ACA}$, latter equality resulting from the isogonality of $\{A_2, D_A\}$. Also for the other angle of this triangle we see that $\widehat{A_2A'B'} = \widehat{A_2CB'} = \widehat{D_ACA'}$, latter equality again due to the same isogonality. However theorem 5 shows (see Figure 16) that $\widehat{D_ACA'} = \widehat{D_ACB} = \widehat{FBC} = \widehat{D_AAC}$. □

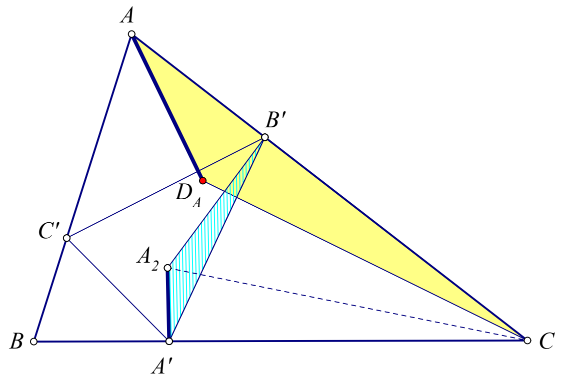

Figure 17: Reduction of the antisimilarity to that of $\triangle A_2A'B'$ to $\triangle D_AAC$

Figure 18 shows the locus κ_A of the center D_2 of the antisimilarity mapping the triangle $A'B'C'$ to $\triangle ABC$. Triangle $A'B'C'$ pivots about the point A_2 and the antisimilarity mapping it to ABC, as we noticed, is the same with the one mapping $\triangle A_2A'B'$ to $\triangle D_AAC$, which, as we noticed in the case of direct similarity in theorem 3, is the same with the one mapping A_2A' to D_AA. In brackets are included the labels appearing in figure 6 of theorem 3 proving that the locus is a conic. The conic passes through certain points, easily found by locating the corresponding positions of the pivoting triangle $A'B'C'$, equivalently, positions of the segment A_2A'. These points are:

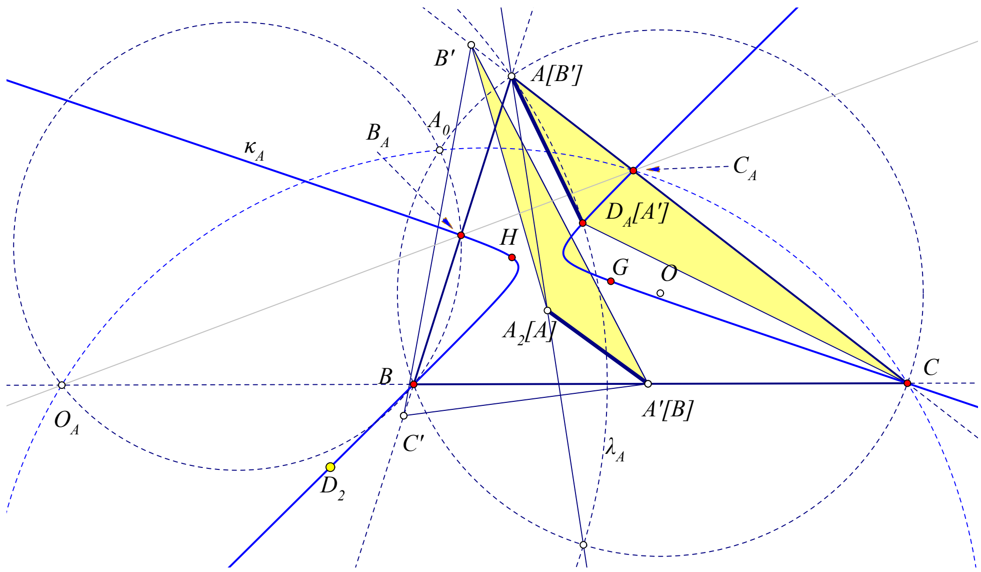

Figure 18: The locus of the antisimilarity centers D_2

1. Point B attained by D_2 when the antisimilarity has its axis identical with the bisector of $\hat{B}$. In this case points $\{B, C', D_2\}$ coincide and the similarity ratio is a/c (see figure 19-(I)).
2. Point C attained by D_2 when the antisimilarity axis is the bisector of $\widehat{C}$. In this case points $\{C, B', D_2\}$ coincide and the similarity ratio is a/b (see figure 19-(II)).
3. Point B_A on side AB being the center of antisimilarity transforming A_2B to D_AA. Its location is determined by the ratio $BB_A/B_AA = A_2B/D_AA$, defining the similar triangles $\{BA_2B_1 \sim AD_AB_A\}$ (see figure 20-(I)). The similarity of the triangles

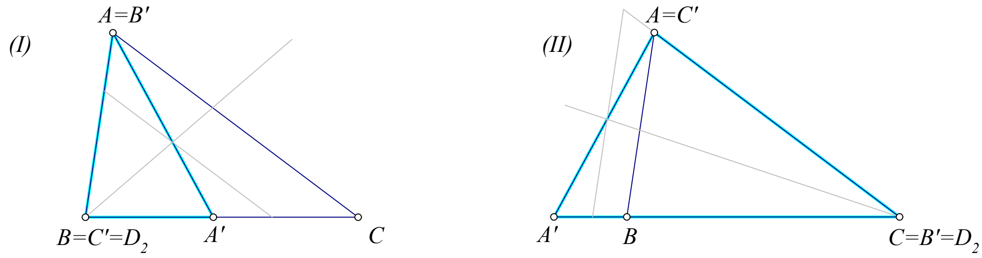

Figure 19: The geometric locus of D_2 contains vertices $\{B, C\}$

results by the equality of the aforementioned ratios and the equality of the angles $\widehat{B_AAD_A} = \widehat{B_ABA_2}$. This in turn follows from the isogonality of $\{A_2, D_A\}$ implying that $\widehat{B_ABA_2} = \widehat{D_ABC}$ and an easy angle chasing argument using figure 16 of theorem 5.

4. Point C_A on side AC being the center of antisimilarity transforming A_2C to D_AA. Its location is determined by the ratio $CC_A/C_AA = A_2C/D_AA$, defining the similar triangles $\{CA_2C_A \sim AD_AC_A\}$ (see figure 20-(II)). The similarity of the triangles provable in exactly the same way as in the preceding *nr*.

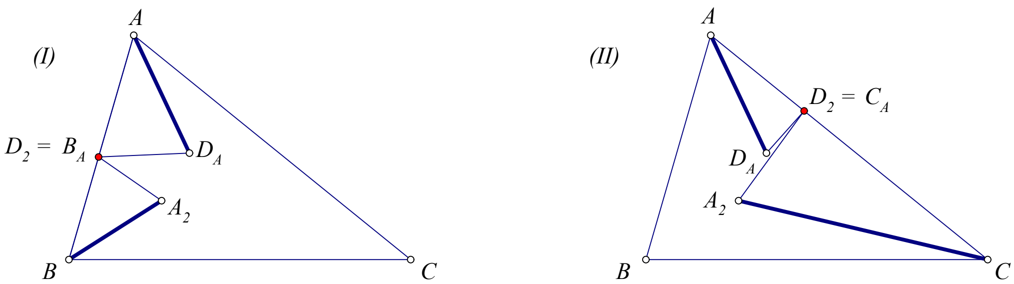

Figure 20: The points $\{B_A \in AB, C_A \in AC\}$ of the geometric locus

5. The centroid G atained as similarity center of the pivoting triangle whose the vertex $A' \in BC$ is the intersection $A' = BC \cap GA_2$. The fact that this is indeed a similarity center follows by showing (see Figure 21) that the ratios $D_AA/D_AG = A_2A'/A_2G$, equivalently the lines $\{AA', A_2D_A\}$ are parallel. This involves a computation in barycentrics w.r.t. $\triangle ABC$, in which the points have the coordinates ([21], [12]):

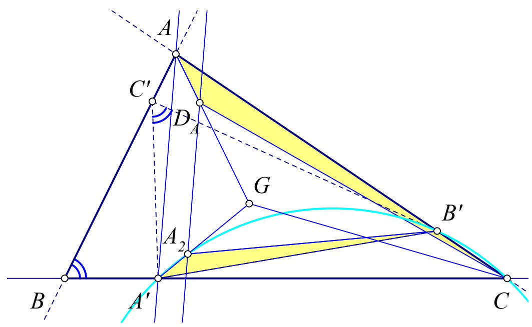

Figure 21: The centroid G as antisimilarity center

$$A(1:0:0)\ ,\ G(1:1:1)\ ,\ A_2(2S_A:b^2:c^2)\ ,\ D_A(a^2:2S_A:2S_A)\ .$$

Here $\{a=|BC|, b=|CA|, c=|AB|\}$ are the side-lengths of the triangle. The symbols $S_A=(b^2+c^2-a^2)/2$, and the analogous expressions resulting by cyclic permutations of the letters are the *"Conway symbols"* ([22]). We use standard methods ([21], [29]) to prove the equality of the aforementioned ratios representing the points in the form

$$A_2 \;=\; \mu\cdot A'+\nu\cdot G \quad \text{and} \quad D_A \;=\; \mu' A+\nu' G$$

and showing that the two ratios are equal:

$$\frac{\nu}{\mu\cdot\sigma_{A'}} \;=\; \frac{\nu'}{\mu'} \;=\; \frac{2S_A}{a^2-2S_A}\ ,$$

where $\sigma_P=u+v+w$ for a point with coordinates $P(u:v:w)$. The calculation details are straightforward and are omitted.

6. The orthocenter H atained when the orthocenter H' of the pivoting triangle coincides with the orthocenter H of $\triangle ABC$. This follows from the following observations:

(6.1) It is well known ([5, p.49], [28, II, p.68]), that as the triangle $A'B'C'$ pivots about A_2 remaining all the time similar to itself, the various points with fixed relative position to it (characterized by constant barycentrics w.r.t. $\triangle A'B'C'$) like its orthocenter, move along lines.

(6.2) For two particular positions of the pivoting triangle $A'B'C'$ the corresponding orthocenters lie on the altitude of $\triangle ABC$. Hence the line carrying the altitudes of all the pivoting $\triangle A'B'C'$ is the altitude AA' of ABC. One such position is obviously that of *nr-1* (see figure 19-(I)), in which one altitude of $A'B'C'$ coincides with one altitude of $\triangle ABC$.

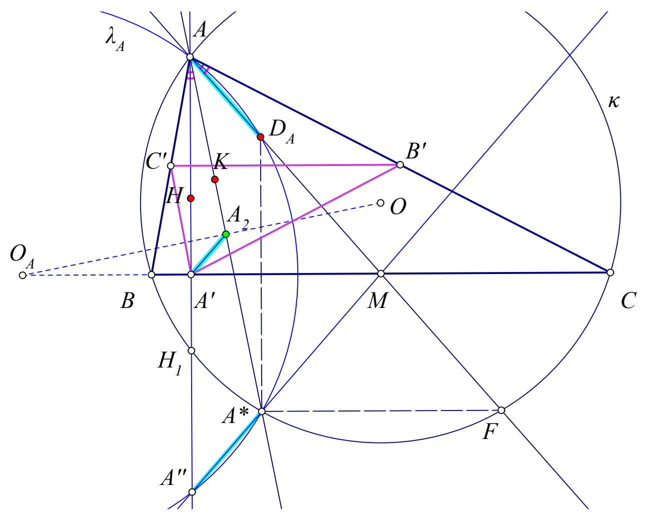

Figure 22: A special position of the pivoting $\triangle A'B'C'$ about A_2

A second position is shown in figure 22. It occurs when A' is the foot of the altitude of $\triangle ABC$ from A. In this case $AD_A=A''A^*=2AA_2$, and the ratio of $\triangle ABC$ to the similar pivoting $A'B'C'$ is two. This implies that $\{A'C'=AB/2\}$ and $A'B'=AC/2$ and consequently $\triangle A'B'C'$ is the reflected of $AB'C'$ on the line $B'C'$ of the middles of the sides of $\triangle ABC$, showing that the orthocenter of $A'B'C'$ is on the line AA'.

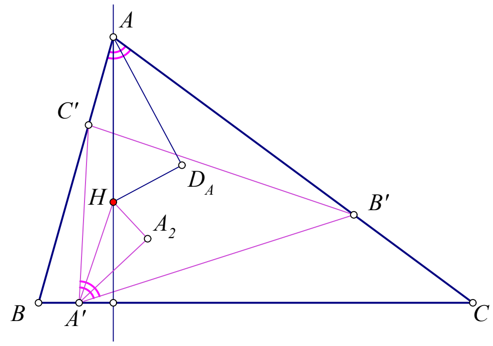

Figure 23: The pivoting $\triangle A'B'C'$ and $\triangle ABC$ with the same orthocenter

(6.3) From the preceding observations follows that there is a position A' for which the corresponding pivoting triangle $A'B'C'$ has its orthocenter identical with the orthocenter H of $\triangle ABC$ (see Figure 23). From the similarity of the two triangles follows then that point H is their antisimilarity center.

7. Finally, from theorem 2 we have that point D_A belongs to the locus under consideration.

Next theorem formulates the discussed properties of the conic κ_A, which analogously hold for the other two conics $\{\kappa_B, \kappa_C\}$ describing the location of the centers of antisimilarities mapping to $\triangle ABC$ the triangles $A'B'C'$ pivoting about one of the other vertices $\{B_2, C_2\}$ of the second Brocard triangle.

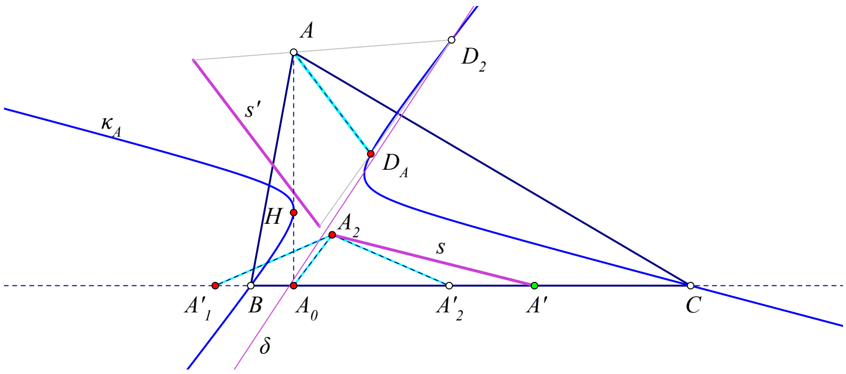

Figure 24: Determination of the direction of the asymptotes of the conic

Theorem 6. *With the notation and conventions used in this section, the conic described by the centers of the antisimilarities mapping the pivoting about A_2 triangle $A'B'C'$ to the triangle of reference ABC is a hyperbola passing through the seven points $\{B, C, B_A, C_A, H, G, D_A\}$. Its asymptotes are parallel to bisectors of the angles formed by the line pairs $\{(D_AA, A_2A_1'), (D_AA, A_2A_2')\}$, where $\{A_1', A_2'\}$ are the points on BC defining equal segments $\{|A_2A_1'| = |A_2A_2'| = |D_AA|\}$ (see Figure 24).*

Proof. We prove the claim about the location of the asymptotes. For this we examine how the antisimilarity with center at D_2 maps the moving segment A_2A' onto D_AA. By the proper definition of the antisimilarity this is done by first reflecting A_2A' on the axis δ of the antisimilarity and then using a homothety centered at D_A. The reflection on δ maps the segment $s = A_2A'$ to a segment s' parallel to D_AA. When the length of s'

approaches the length of D_AA the homothety center D_2 of the two segments $\{s', D_AA\}$ tends to infinity, showing that the conic extends to infinity. The argument shows also that the direction of the asymptote is the limiting position of δ, which is indeed the direction of a bisector of the angle formed by the lines $\{A_2A'_2, D_AA\}$.

The question of the *existence* of two such segments $\{A_2A'_1, A_2A'_2\}$ with lengths equal to $|D_AA|$ is answered by the observation made in (6.2). There we saw that the distance of A_2 from the foot A_0 of the altitude from A is $|A_2A_0| = |D_AA|/2$. Hence the distance of A_2 from BC is less than $|D_AA|/2$ thereby proving the existence of precisely two points $\{A'_1, A'_2\}$ on BC with the claimed property. □

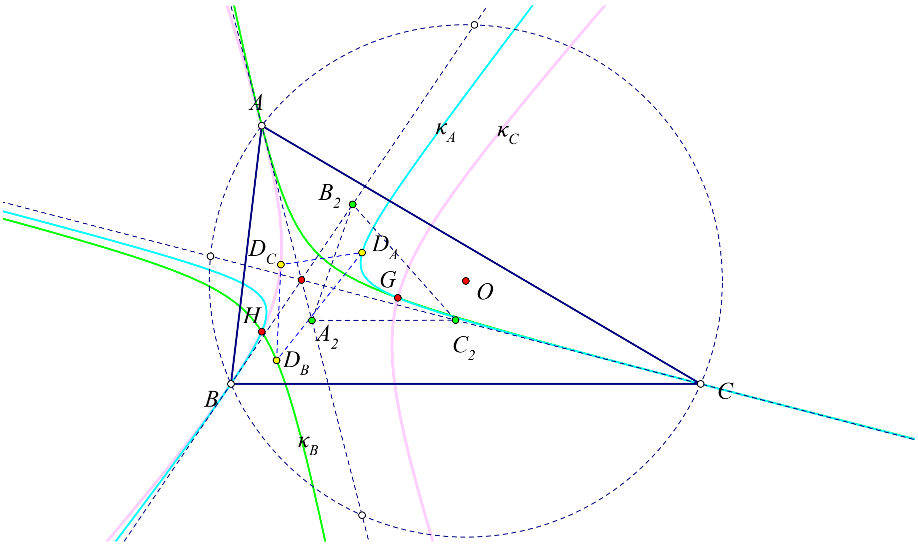

Figure 25: The three hyperbolas $\{\kappa_A, \kappa_B, \kappa_C\}$

9 Pivoting about the inverses of the Brocard points

In this section we'll discuss in some detail the case of the inverse Ω^* w.r.t. the circumcircle of $\triangle ABC$ of the first Brocard point Ω. The configuration for the inverse Ω'^* of the second Brocard point is completely analogous and we'll describe in brief the corresponding steps and point out the relations between the two resulting conics κ_Ω and $\kappa_{\Omega'}$.

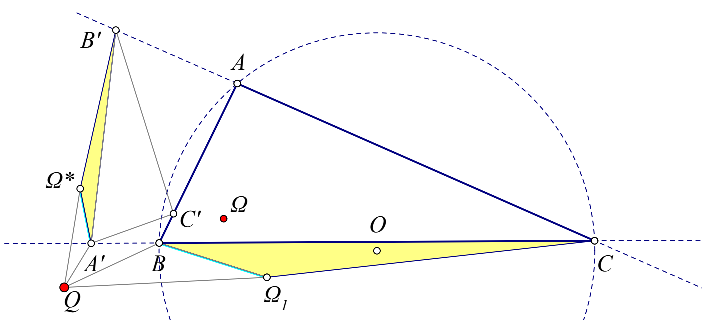

Figure 26: $\triangle A'B'C'$ pivoting about the inverse Ω^* of the first Brocard point Ω

The pivoting triangles $\triangle A'B'C'$ about Ω^* are antisimilar to $\triangle ABC$ and the antisimilarity carrying $\triangle ABC$ to $\triangle A'B'C'$, as we saw also in the previous cases, is identical to the antisimilarity carrying the fixed segment Ω_1B to the variable Ω^*A' (see Figure 26).

The variable segment Ω^*A' joins the pivot center to the vertex $A' \in BC$ of the pivoting triangle. Under the considered similarity point Ω^* corresponds to a fixed point Ω_1 such that $\Omega^*A'B'$ and Ω_1BC are triangles corresponding under this antisimilarity. The selection of the pair of segments (Ω^*A', Ω_1B) is arbitrary, and we could equally well come to the same results by selecting one of the other pairs $\{(\Omega^*C', \Omega_1A)\ ,\ (\Omega^*B', \Omega_1C)\}$ corresponding under the similarity. The figure shows also the center Q of the (anti)similarity mapping $\triangle ABC$ to $\triangle A'B'C'$ and also $\triangle\Omega_1BC$ to $\triangle\Omega^*A'B'$.

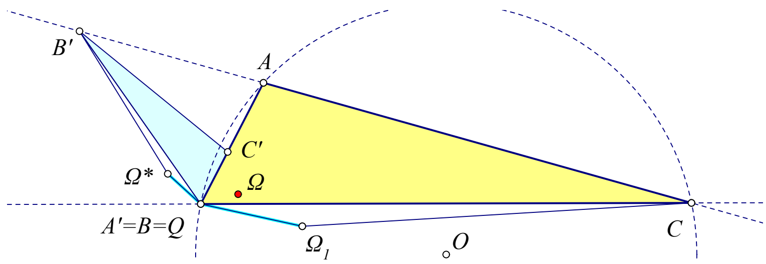

Figure 27: Position of $\triangle A'B'C'$ for which $Q = A' = B$

From theorem 2 we know that the centers Q of the antisimilarities mapping $\triangle ABC$ to $\triangle A'B'C'$ describe a conic κ_Ω passing also through the point Ω_1. We can easily see that the conic passes also through the vertices of the triangle ABC. Figure 27 shows the special position of the pivoting triangle for which the corresponding antisimilarity center coincides with B. Figure 28 shows the two other cases, in which we reduce the antisimilarity to that of the pair of segments (Ω^*C', Ω_1A) (Figure 28-I) and (Ω^*B', Ω_1C) (Figure 28-II). The figures show the positions of the pivoting triangle for which the antisimilarity center coincides with the vertices $\{A, C\}$ of the triangle of reference. They illustrate the fact that κ_Ω is a *"triangle conic"*, i.e. a conic passing through the vertices of the triangle of reference.

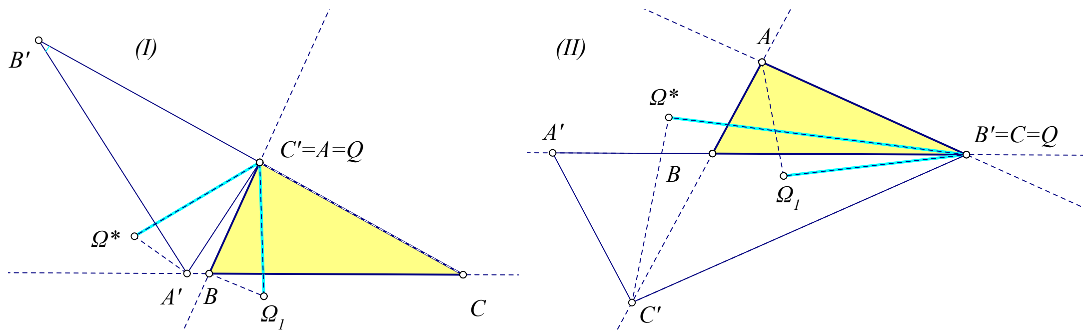

Figure 28: Positions of pivoting $\triangle A'B'C'$ for which $Q = A$ and $Q = C$

From theorem 2 we know that this conic passes also through point Ω_1 and in the following lines we deal with two other points also contained in this conic, which will help us determine the line, whose isogonal image is κ_Ω. The first of these, Q_0, is the second point of the conic κ_Ω contained in the line $\Omega^*\Omega_1$. The second is the *"Tarry point"* T ($X(98)$ in Kimberling's notation for *"triangle centers"* [18], [4]) of $\triangle ABC$, proved to be the fourth intersection point of the conic with the circumcircle κ of $\triangle ABC$ (see Figure 29). Point Q_0 has a simple geometric construction based on the proper definition of the antisimilarity.

Lemma 2. *With the notation and conventions of this section, point Q_0 can be constructed using only ruler and compass.*

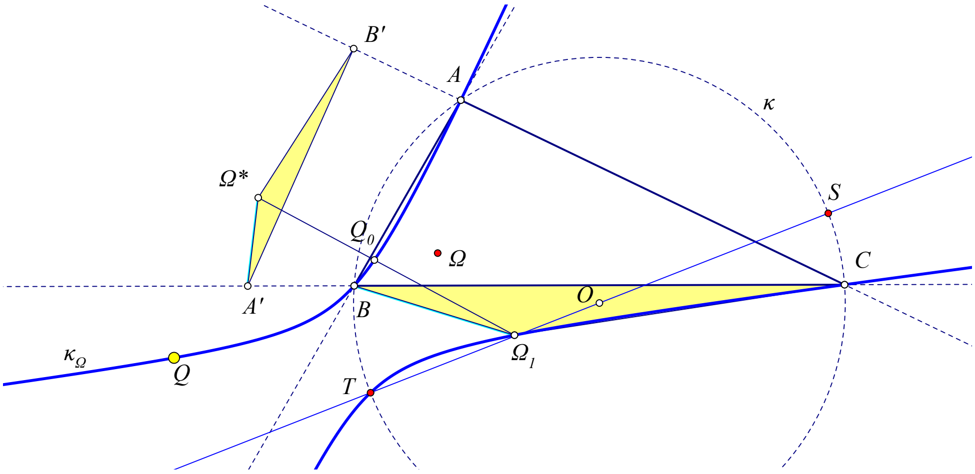

Figure 29: The conic κ_Ω and the points $\{Q_0, T\}$

Proof. In fact, by its definition, Q_0 defines two antisimilar triangles $\{Q_0\Omega^*A', Q_0\Omega_1 B\}$ with $A' \in BC$ (see Figure 30). The antisimilarity relating these triangles has an axis bisecting the angle $\Omega^*\widehat{Q_0}\Omega_1$, hence in this case it is a line Q_0D orthogonal to line $\Omega^*\Omega_1$. Thus, point $Q_0 \in \Omega^*\Omega_1$ has the two properties: (i) $Q_0\Omega^*/Q_0\Omega_1 = Q_0A'/Q_0B$ and (ii) Q_0D bisects the angle $B\widehat{Q_0}A'$. Reflecting A' in the line $\Omega^*\Omega_1$ to the point F we obtain the collinear points $\{B, Q_0, F\}$ and the relation $FQ_0/Q_0B = \Omega^*Q_0/Q_0\Omega_1$. This implies that the line $\varepsilon = \Omega^*F$ is parallel to $B\Omega_1$ and F lies also on the reflected line δ of BC w.r.t. line $\Omega^*\Omega_1$. Thus, it coincides with the intersection $F = \varepsilon \cap \delta$ of two known lines and $Q_0 = BF \cap \Omega^*\Omega_1$. □

This construction leads to the determination of the barycentrics of Q_0, which together with analogous determination of the barycentrics of $\{\Omega^*, \Omega_1, \Omega'^*, \Omega'_1\}$, is formulated through the next lemma.

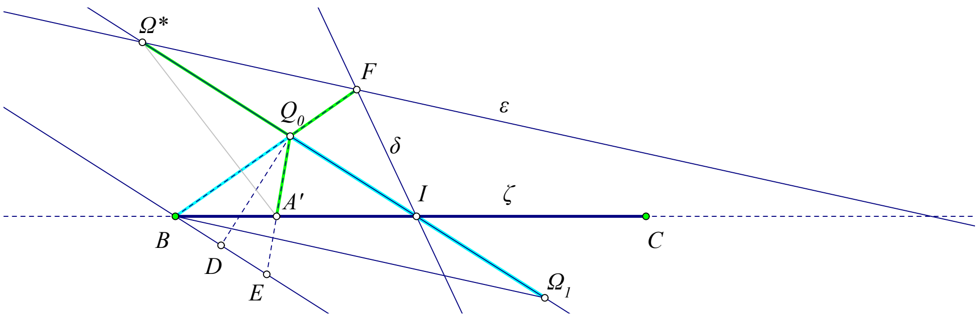

Figure 30: Construction of the point Q_0

Lemma 3. *The barycentrics of the following points w.r.t. the triangle ABC are:*

$$\Omega^* = ((S_B + S_C)(S_B - S_A) : \dots : \dots), \tag{6}$$

$$\Omega_1 = ((S_B - S_C)(S_B - S_A) : \dots : \dots), \tag{7}$$

$$\Omega'^* = ((S_B + S_C)(S_C - S_A) : \dots : \dots), \tag{8}$$

$$\Omega'_1 = ((S_C - S_A)(S_C - S_B) : \dots : \dots), \tag{9}$$

$$Q_0 = \left(\frac{S_B}{(S_C - S_B)(S_A^2 - S_B S_C)} : \dots : \dots \right). \tag{10}$$

the dots standing for the other coordinates resulting by cyclic permutations of the letters $\{A, B, C\}$.

Proof. A proof of (6) results by considering the $\kappa-$inverse Ω^* of Ω as intersection of the *"Lemoine line"* ε and the line $O\Omega$ (see Figure 31). The Lemoine line $\frac{u}{a^2} + \frac{v}{b^2} + \frac{w}{c^2} = 0$ is

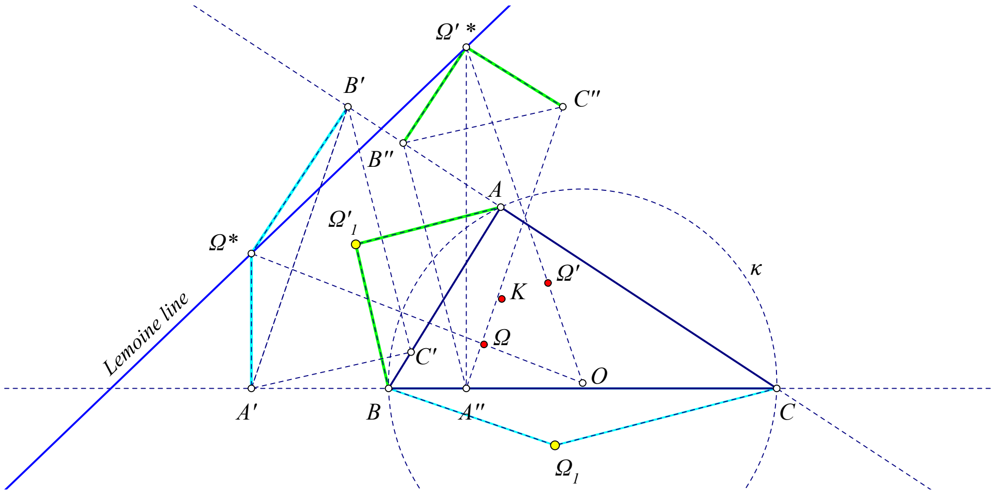

Figure 31: The points $\{\Omega^*, \Omega'^*\}$ and $\{\Omega_1, \Omega'_1\}$

the *"trilinear polar"* of the symmedian point $K(a^2 : b^2 : c^2)$ and the coefficients of the line $O\Omega$ are determined by the vector product $(a^2S_A : b^2S_B : c^2S_C) \times (1/a^2 : 1/b^2 : 1/c^2)$ of the barycentrics of the two points.

The coordinates of Ω_1 are determined by considering the matrix M expressing the antisimilarity f mapping $\triangle ABC$ onto the pedal $\triangle A'B'C'$ of Ω^*. The correspondence is

$$A \overset{f}{\mapsto} C' \in AB : (c^4 + a^4 - b^2(c^2 + a^2) \ : \ (c^2 - a^2)^2 - b^2(c^2 + a^2) + 2b^4 \ : \ 0),$$

$$B \overset{f}{\mapsto} A' \in BC : (0 \ : \ a^4 + b^4 - c^2(a^2 + b^2) \ : \ (a^2 - b^2)^2 - c^2(a^2 + b^2) + 2c^4),$$

$$C \overset{f}{\mapsto} B' \in CA : ((b^2 - c^2)^2 - a^2(b^2 + c^2) + 2a^4 \ : \ 0 \ : \ b^4 + c^4 - a^2(b^2 + c^2)).$$

The matrix M has the above rows as columns and the coordinates $\{Y, X\}$ of $\{\Omega^*, \Omega_1\}$ are related by the linear equations $Y = MX$. Having Y from equation (6) and solving for X we find $X = ((a^2 - b^2)(c^2 - b^2) : (b^2 - c^2)(a^2 - c^2) : (c^2 - a^2)(b^2 - a^2))$, which is equivalent to (7).

A similar reasoning with minor modifications proves the equalities (8) and (9).

Finally, the coordinates of Q_0 in equation (10) result by expressing its geometric construction in barycentrics. The calculations involve the determination of the reflection of a line in another line and repeated standard applications of the vector product of pairs of vectors of barycentrics which I omit.

By the way, referring to figure 31, I notice that the two pedals $\{\triangle A'B'C', \triangle A''B''C''\}$ of the points $\{\Omega^*, \Omega'^*\}$ are congruent by a point-symmetry. This is true also for their pivots by the same angle ϕ, the corresponding symmetry center moving on a fixed line as ϕ varies. □

Corollary 2. *The points* $\{\Omega_1, \Omega'_1\}$ *are respectively isogonal conjugate to* $\{\Omega'^*, \Omega^*\}$.

Proof. This is immediately seen by applying the isogonal transformation, using its representation $Y(u' : v' : w') = I(X(u : v : w))$ in the form

$$(u' : v' : w') \ = \ (\ (S_B + S_C)/u \ : \ (S_C + S_A)/v \ : \ (S_A + S_B)/w\ ). \qquad \square$$

Theorem 7. *The Tarry point T of the triangle ABC is contained in the conic κ_{Ω}.*

Proof. Since the triangle conic κ_{Ω} passes through the points $\{\Omega_1, Q_0\}$, it is the isogonal conjugate of the line ε_{Ω} through the isogonal conjugates $\{I(\Omega_1) = \Omega'^*, I(Q_0)\}$ of these points. Thus, it suffices to show that the isogonal conjugate $I(T)$ of the Tarry point satisfies the equation of the line ε_{Ω}. The coefficients of this line are determined by the vector product of the corresponding barycentrics of $\{\Omega'^*, I(Q_0)\}$:

$$\varepsilon_{\Omega} = \left(\frac{S_B}{S_B + S_C} : \frac{S_C}{S_C + S_A} : \frac{S_A}{S_A + S_B} \right), \tag{11}$$

and the claim is readily verified using the coordinates of T ([18]) in the form

$$T(\, 1/(S_A^2 - S_B S_C) \,:\, 1/(S_B^2 - S_C S_A) \,:\, 1/(S_C^2 - S_A S_B)\,)\,.$$

□

Theorem 8. *The triangle conic κ_{Ω} has perspector the point $(S_B : S_C : S_A)$ and satisfies the equation*

$$S_B vw + S_C wu + S_A uv = 0\,. \tag{12}$$

It is the isogonal conjugate of the line ε_{Ω} which intersects the Lemoine line orthogonally at the point Ω'^*.

Proof. Since the conic is the isogonal cojugate of ε_{Ω}, its equation results from equation (11), showing also that $(S_B : S_C : S_A)$ is its perspector, producing the conic through the tripoles of the lines passing through it ([29, p.114]).

Regarding the orthogonality, it suffices to show that the directions of the Lemoine line and ε_{Ω} are orthogonal. Since the Tarry point is on the circumcircle κ, its isogonal $I(T)$ is at infinity and determines the *"direction"* of the line ε_{Ω}. Thus, it suffices to verify the orthogonality condition ([29, p.54]):

$$S_A pp' + S_B qq' + S_C rr' = 0\,, \tag{13}$$

for $I(T)$ and the point at infinity of the Lemoine line:

$$I(T) = (p : q : r) = (\, (S_B + S_C)(S_A^2 - S_B S_C) \,:\, \ldots \,:\, \ldots\,), \tag{14}$$

$$\text{Lemoine inf.:}\ (p', q', r') = (\, (S_B^2 - S_C^2) \,:\, \ldots \,:\, \ldots\,), \tag{15}$$

which is indeed easily verified. □

The study of the centers of the antisimilarities mapping the pivoting triangle $A''B''C''$ about the κ−inverse Ω'^* of the second Brocard point Ω' follows the same line of reasoning and leads to the analogous conic $\kappa_{\Omega'}$ and the following theorem.

Theorem 9. *The triangle conic $\kappa_{\Omega'}$ has perspector the point $(S_C : S_A : S_B)$ and satisfies the equation*

$$S_C vw + S_A wu + S_B uv = 0\,. \tag{16}$$

It is the isogonal conjugate of the line $\varepsilon_{\Omega'}$ which intersects the Lemoine line orthogonally at the point Ω^*.

Figure 32 shows the conics $\{\kappa_\Omega, \kappa_{\Omega'}\}$ and their corresponding isogonal lines $\{\varepsilon_\Omega, \varepsilon_{\Omega'}\}$. Latter, because of the symmetry of $\{\Omega^*, \Omega'^*\}$ w.r.t. to the *"Brocard axis"* OK lie symmetrically w.r.t. the circumcenter O. Thus, since the kind of the conic depends on the number of intersection points of the lines $\{\varepsilon_\Omega, \varepsilon_{\Omega'}\}$ with the circle, they are always of the same kind: hyperbolas if these lines intersect the circle in two points, parabolas if they touch it and ellipses if they have no real intersection points with the circumcircle. It is also well known ([11, p.80]), that in the case the isogonal line of a triangle conic (hyperbola) λ intersects the circumcircle at two points $\{X, Y\}$, then the *Wallace-Simson* (WS-) lines $\{w_X, w_Y\}$ of these points are orthogonal to the asymptotic directions of λ. This implies that the asymptotes $\{v', w'\}$ of κ_Ω are parallel to the WS-lines of the intersections $\{V', W'\}$ of $\varepsilon_{\Omega'}$

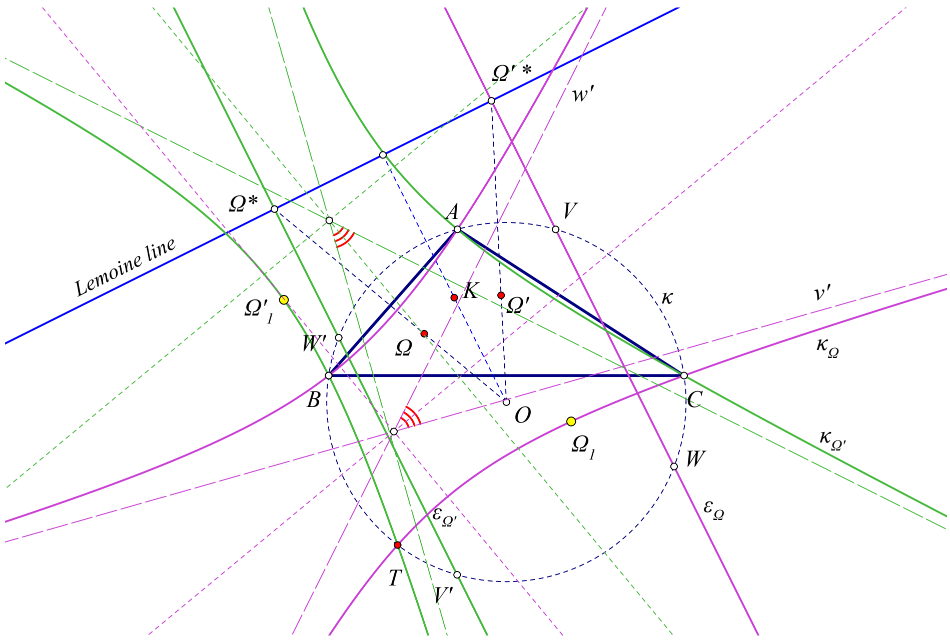

Figure 32: The conics $\{\kappa_\Omega, \kappa_{\Omega'}\}$ and their isogonal lines $\{\varepsilon_\Omega, \varepsilon_{\Omega'}\}$

with κ, that the angles of the asymptotes of the two conics are equal and that the axes of the two conics are pairwise parallel. Latter is a property for any pair of conics passing through four fixed points $\{A_i, i = 1..4\}$ lying on a circle. In fact, by a well known property ([19, I, p.372]), the axes of the conics are then parallel to the bisectors of the angles formed by any two chords of the circle joining two of the $\{A_i\}$ and having no common end points.

Figure 33 shows the case in which the lines $\{\varepsilon_\Omega, \varepsilon_{\Omega'}\}$ are tangent to the circumcircle, their isogonals producing then two parabolas. This determines a special Brocard angle ω_0 such that $\sin(\omega_0) = R/|O\Omega'^*|$, where R the circumradius of $\triangle ABC$. Every triangle having this Brocard angle will have necessarily corresponding conics $\{\kappa_\Omega, \kappa_{\Omega'}\}$ parabolic. Notice that in this case the four points $\{A, B, C, T\}$ suffice for their determination, since by four points in general position pass at most two parabolas ([22]). The preceding relation for the Brocard angle is easily seen to be equivalent with the condition:

$$\sin(\omega_0) = \frac{1}{\sqrt{5}} \quad \Leftrightarrow \quad \omega_0 \approx 26^\circ : 33' : 54'' .$$

More general, considering the projection J of O on ε_Ω and setting $k = OJ^2/R^2$ we see, by a short calculation of distances expressed in barycentrics, that

$$\sin^2(\omega) = \frac{1}{4 + \frac{1}{k}} .$$

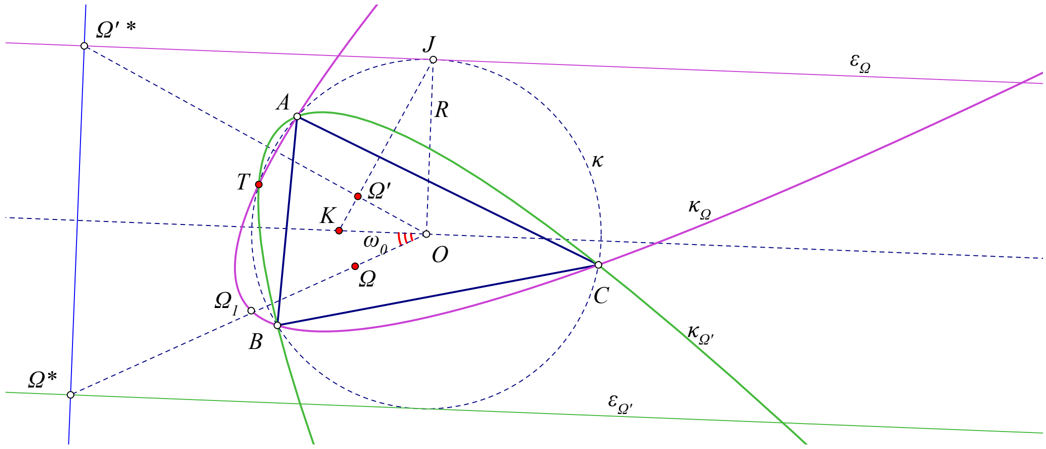

Figure 33: Case in which $\{\kappa_{\Omega}, \kappa_{\Omega'}\}$ are parabolas

Thus, for $\{OJ > R \Leftrightarrow k > 1 \Leftrightarrow \omega > \omega_0\}$ the two conics are ellipses, whereas if $\omega < \omega_0$ they are hyperbolas. We recapitulate the preceding discussion as a theorem.

Theorem 10. *The conics $\{\kappa_{\Omega}, \kappa_{\Omega'}\}$, carrying the centers of antisimilarities mapping pivoting triangles correspondingly about $\{\Omega^*, \Omega'^*\}$ to $\triangle ABC$, are isogonal images of the lines $\{\varepsilon_{\Omega}, \varepsilon_{\Omega'}\}$, which are orthogonal to the Lemoine line respectively at $\{\Omega'^*, \Omega^*\}$. The conics pass through the Tarry point T of $\triangle ABC$ and are hyperbolas, parabolas or ellipses when the Brocard angle ω of $\triangle ABC$ is correspondingly $\{\omega < \omega_0, \omega = \omega_0, \omega > \omega_0\}$.*

Bibliography

[1] Barker, W. and Hove, R., *Continuous Symmetry, From Euclid to Klein*, American Mathematical Society, New York, 2007.

[2] Bradley, C. and Smith, R., *The Locations of the Brocard Points*, Forum Geometricorum, **6 (2006)**, 71-77.

[3] Casey, J., *A treatise on the analytical geometry of the point, line, circle and conic sections*, Hodges Figgis and Co., Dublin, 1893.

[4] Clawson, W., *Points on the Circumcircle*, American Mathematical Monthly, **32 (1925)**, 169-174.

[5] Court, G., *College Geometry*, Dover Publications Inc., New York, 1980.

[6] Coxeter, H., *Introduction to Geometry*, John Wiley and Sons Inc., New York, 1961.

[7] Deaux, R., *Introduction to the Geometry of Complex Numbers*, Dover, New York, 1956.

[8] Droussent, L., *On the Orthocentroidal Circle*, American Mathematical Monthly, **57 (1950)**, 169-171.

[9] Eiden, J., *Geometrie Analytique Classique*, Calvage - Mounet, Paris, 2009.

[10] Franzsen, W., *The Distance from the Incenter to the Euler Line*, Forum Geometricorum, **11 (2011)**, 231-236.

[11] Gallatly, W., *The modern geometry of the triangle*, F. Hodgsonn, London, 1913.

[12] Gibert, B., *Brocard triangles*, https://bernard-gibert.pagesperso-orange.fr/gloss/brocardtriangles.html, 2021.

[13] Glaeser, G. and Stachel, H. and Odehnal, B., *The universe of conics*,Springer, Berlin, 2016.

[14] Guinand, A., *Euler Lines, Tritangent Centers, and Their Triangles*, American Mathematical Monthly, **91 (1984)**, 290-300.

[15] Hahn, L., *Complex Numbers and Geometry*, Mathematical Association of America, Washington, 1994.

[16] Honsberger, R., *Episodes in Nineteenth and Twentieth Century Euclidean Geometry*, Mathematical Association of America, Washington, 1995.

[17] Johnson, R., *Advanced Euclidean Geometry*, Dover Publications Inc., New York, 1960.

[18] Kimberling, K., *Encyclopedia of Triangle Centers*, http://faculty.evansville.edu/ck6/encyclopedia/ETC.html, 2018.

[19] Loney, S., *The elements of coordinate geometry I, II*, AITBS publishers, Delhi, 1991.

[20] Pamfilos, P., *A Gallery of Conics by Five Elements*, Forum Geometricorum, **14 (2014)**, 295-348.

[21] Pamfilos, P., *Barycentric coordinates*, http://users.math.uoc.gr/~pamfilos/eGallery/problems/Barycentrics.pdf, 2019.

[22] Pamfilos, P., *Conway triangle symbols*, http://users.math.uoc.gr/~pamfilos/eGallery/problems/Conway.pdf, 2019.

[23] Pamfilos, P., *Similarities*, http://users.math.uoc.gr/~pamfilos/eGallery /problems/Similarities.pdf, 2019.

[24] Pamfilos, P., *Symmedian*, http://users.math.uoc.gr/~pamfilos/eGallery /problems/Symmedian.pdf, 2019.

[25] Pamfilos, P., *Pedals of triangles*, http://users.math.uoc.gr/~pamfilos/eGallery /problems/Pedals.pdf, 2019.

[26] Schwerdtfeger, H., *Geometry of complex numbers*, Dover, New York, 1979.

[27] Snyder, W., *Selected topics in algebraic geometry I+II*, Chelsea, New York, 1970.

[28] Yaglom, I., *Geometric Transformations I, II, III, IV*, Mathematical Association of America, Washington, 1962.

[29] Yiu, P., *Introduction to the Geometry of the Triangle*, http://math.fau.edu/Yiu/Geometry.pdf, 2013.

DEPARTMENT OF MATHEMATICS
AND APPLIED MATHEMATICS
UNIVERSITY OF CRETE
HERAKLION, 70013 GR
E-mail address: pamfilos@uoc.gr